2

Nanophotonic Emission Control for Improved Photovoltaic Efficiency

With the necessary transition to renewable energy at hand, there is a renewed research focus on increasing solar cell efficiency, in order to reduce the cost of electricity. Nanomaterials are promising candidates to contribute to a new generation of low cost and highly efficient solar cells. Due to their wavelength-scale dimensions, nanomaterials display exceptionally strong light-matter interactions that lead to large perturbations in absorption and emission compared to their bulk counterparts. Although most work on nanostructured solar cells has focused on increasing the absorption, emission control may have even greater potential for improving efficiency of state-of-the-art solar cells. In this chapter, we describe how nanostructures can be applied to improve solar cell efficiency, focusing on emission control. First, we analyze the requirements for making the most efficient solar cell, by looking at the thermodynamics of energy conversion. We show that an ideal solar cell at open circuit displays emission that is identical to its absorption. Comparing this to the emission of a typical silicon solar cell shows that there are three differences: the intensity, the angles in which light is emitted, and the spectrum. These differences lead to a reduction in efficiency, mainly due to a drop in open circuit voltage. For each loss mechanism, we discuss how nanomaterials can manipulate the emission and thereby reduce the voltage loss. Finally, we analyze the performance of two conceptual designs for solar cells based on nanomaterials. These give a large improvement in efficiency compared to conventional designs, showing the great potential of nanomaterials in solar cells.

2.1 INTRODUCTION

Over the past decades, the price of electricity generated by solar panels dropped drastically.[15] However, to become fully competitive with fossil fuels, including the cost of energy storage, electricity from solar panels has to become even cheaper. The materials, manufacturing and installation costs are already pushed to their lower limit, but by increasing the electricity output per panel, the price of energy can be reduced further.[16,17] This requires an increase in solar cell efficiency.

Nanomaterials display exceptionally strong light-matter interactions and are therefore promising candidates to consider for the next generation of high efficiency solar cells.[10,18,19] The close matching between the wavelength of light and the size of nanomaterials can lead to a variety of resonant effects.[18] By controlling their shape and size, nanomaterials offer greatly enhanced flexibility in tuning the angle, wavelength and rate of both absorbed and emitted photons compared to their bulk counterparts.[20,21] This so-called nanophotonic engineering allows for optimizing the optical properties for application in solar cells.

Initially most research in the field of nanophotonics for solar cells was focused on maximizing light absorption. Nanomaterials can act as optical antennas, concentrating light from an area much larger than their physical size, leading to greatly enhanced absorption. The electrical current generated by a solar cell scales with the number of absorbed photons, and the optimization of light absorption has led to short circuit currents (J_{sc}) close to the theoretical maximum.[10] The open circuit voltage (V_{oc}) of solar cells, however, was mostly seen as a consequence of material properties, design architecture and fabrication, and was less considered as an optical problem.

It can be shown however, that nanophotonic engineering can also improve the open circuit voltage, by optimizing light emission of the solar cell. The connection between optimizing light absorption and increasing current is very clear, but optimization of light management for high V_{oc} is less intuitive. Although the importance of emission control was already recognized by Shockley and Queisser in their seminal paper on solar cell efficiency[22] and later discussed in more detail several decades ago,[23] practical implementation has been limited. Improvements have been made, but the achieved open circuit voltages are still further away from the theoretical limit[10] than the achieved J_{sc}. The only exception is Gallium-Arsenide (GaAs) solar cells, which have been studied for their outstanding optical properties for a long time.

Most early work on emission control was based on angle restriction filters, that block emission into certain angles. Only recently nanophotonic strategies started to be implemented that allow for a fundamentally different approach, with the key difference being the stage at which the emission is controlled. Angle restriction filters, even if they are based on nanoscale structures like Bragg stacks or photonic crystals,[24,25,26] interact with the light after it has been emitted. Nanophotonic engineering changes the photonic environment of the emitter, and thereby the emission process itself. This is particularly relevant for non-ideal materials, where non-radiative recombination is dominant. With angle restrictors the light emitted at oblique angles is reflected back, which leads to an increase of photon recycling, i.e. reabsorption of emitted photons. This reabsorption enhances the non-radiative recombination. In any practical application, this increase in non-radiative recombination nullifies any increase in efficiency coming from angle restriction.[27] This led to the general idea that emission control only helps for materials close to the radiative

limit. However, nanophotonic structures enable emission control while simultaneously reducing non-radiative recombination.[21,28,29,30,20] In this perspective paper we will give an overview of how nanophotonic engineering can be used to increase solar cell efficiency, with a focus on increasing the open circuit voltage, by exploring the opportunities arising from light-matter interactions at the nanoscale that are fundamentally different from any bulk phenomena.

This perspective article is structured as follows. We start with deriving the theoretical maximum efficiency for converting solar energy to electrical power. This derivation gives insight in why light emission is an important performance parameter for solar cells and shows us how an ideal solar cell should perform. From this theoretical maximally efficient solar cell we can find three aspects in which any real solar cell differs from the ideal one. These lead to three loss mechanisms that limit the efficiency of solar cells. For each of these, we will discuss nanophotonics strategies that can be applied to minimize the losses. Finally, we will present two designs for high efficiency solar cells, based on the proposed techniques, and we analyze the performance modeled under realistic operation conditions. We discuss the (optical) properties required for such cells and highlight some of the most important research questions that still need to be addressed.

2.2 Fundamentals of photovoltaics

The upper limit on the conversion efficiency of solar to electrical energy is set by the first and second law of thermodynamics. These laws have played a major role in the development of any energy technology we have today. Applying them to solar energy conversion, will give insight in how we can approach the upper limit of efficiency. In the thermodynamic model, the photovoltaic (PV) system acts as a heat engine, with the sun as the hot source, the ambient as the cold source and the light as heat exchange medium. Optimizing a heat engine requires optimizing the heat exchange. In the case of PV this means optimizing the light management is a way to improve efficiency. Understanding how a PV system should operate from a thermodynamics point of view, gives insight in how we should manage the light with nanophotonics.

When a heat engine extracts heat from a hot source at T_H, not all energy can be converted into useful work. Since work is free of entropy, the entropy from the hot source has to go somewhere else, which requires some heat to be lost towards a cold sink at T_C. The maximum efficiency of this heat engine is given by the Carnot limit:

$$\eta_{carnot} = 1 - \frac{T_C}{T_H}. \tag{2.1}$$

With the sun at T_H=6000K and the ambient at T_C=300K, the maximum efficiency is 95%.

This limit can be reached in theory with the following requirements: the PV system consists of an infinite stack of solar cells with smoothly varying bandgap from 0 to ∞ with full absorption and without the presence of any non-radiative recombination and etendue expansion.[31] The performance of such a system can be derived, based on the fact that any material at non-zero temperature must exchange thermal radiation with the environment to be in thermal equilibrium. According to Kirchhoff's reciprocity law, absorption and emission at a given wavelength, into a given angle are always coupled.[32] The emission (and thus absorption) spectrum of an ideal black body is described by Planck's law and is a

function of temperature. The incident flux of photons with energy E on a solar cell coming from the sun at temperature T_S is:

$$f_i = \frac{1}{exp\left(\frac{E}{k_B T_S}\right) - 1} \frac{2\pi E^2}{h^3 c^2}, \tag{2.2}$$

with h being Planck's constant, q the elemental charge, k_B Boltzmann's constant and c the speed of light. Note that this equation assumes illumination from the full hemisphere or full concentration, corresponding to no etendue expansion between emission and absorption. When a voltage builds up in a material, the emission intensity is increased. The flux of photons f_0 emitted by a solar cell at energy E depends on the temperature T_C and the voltage V over the cell according to:

$$f_0 = \frac{1}{exp\left(\frac{E-qV}{k_B T_C}\right) - 1} \frac{2\pi E^2}{h^3 c^2}. \tag{2.3}$$

This equation gives the photon flux emitted by each cell with a bandgap at E in the infinite stack of cells.[31] In open circuit, when no electrical current is extracted from the cell, the emitted and absorbed photon flux must balance to reach thermal equilibrium. The emission spectrum of the infinite stack of solar cells then equals the emission spectrum of the sun, meaning that $f_0 = f_i$ at every E, which requires:

$$\frac{E - qV_{oc}}{k_B T_C} = \frac{E}{k_B T_S} \tag{2.4}$$

Where V_{oc} is the open circuit voltage in each cell. This can be rewritten to:

$$\frac{qV_{oc}}{E} = 1 - \frac{T_C}{T_S} = \eta_{carnot}, \tag{2.5}$$

which gives a direct relation between the theoretical maximum V_{oc} in each cell and the Carnot limit. It shows that the energy of the photons (E) is converted to energy of electrons (qV_{oc}) with the Carnot efficiency.

From this derivation, we can conclude that to optimize solar cell performance, the emission spectrum at V_{oc} must approach that of the sun. In a practical solar cell, three effects cause the emission spectrum to differ from the solar spectrum and thereby reduce efficiency. First of all, a practical solar cell consists of a limited number of materials, often only one. A single bandgap material has a narrow emission spectrum, that peaks close to the bandgap and exponentially decreases towards higher energy. The second effect is the difference between absorption and emission angles. In the derivation above, emission and absorption happen in the same solid angle. In practice, a cell receives collimated sunlight over a narrow angle, while it emits in all directions. This increase in etendue can be seen as a heat loss towards the environment or as an increase in photon entropy. Finally, any real material provides non-radiative pathways, via which absorbed photons are lost as heat towards the environment. This reduces the emission intensity compared to the incoming sunlight.

To extract power, current must be drawn. This moves the system away from the reversible Carnot limit and reduces the maximum efficiency. Excited states now do work instead of emitting light, which reduces the emission intensity. The resulting maximum power conversion efficiency is 87%.[31] It is important to make the distinction between this useful reduction in voltage and the three mechanisms mentioned above, which decrease the voltage without increasing the current.

The well known Shockley-Queisser limit[22] is also based on thermodynamics, but for a less idealized system. It includes two of the three loss mechanisms: it assumes a single stepwise bandgap and takes into account the difference in solid angle between emission and absorption, but it does not include non-radiative recombination. The system is characterized by the short circuit current density J_{sc}, which is the same as the photo-generated current density, and the dark current density J_0, which is the recombination current density in the dark. These two determine the open circuit voltage V_{oc} according to[33]

$$V_{oc} = \frac{k_B T}{q} ln\left(\frac{J_{sc}}{J_0}\right). \tag{2.6}$$

With these assumptions, the efficiency as a function of bandgap can be calculated, shown as the red line in figure 2.1. This calculation uses the AM1.5G spectrum with 1 sun illumination. It has a maximum efficiency of 34%, which is far below the limit of 87% due to the emission being narrowband and isotropic.

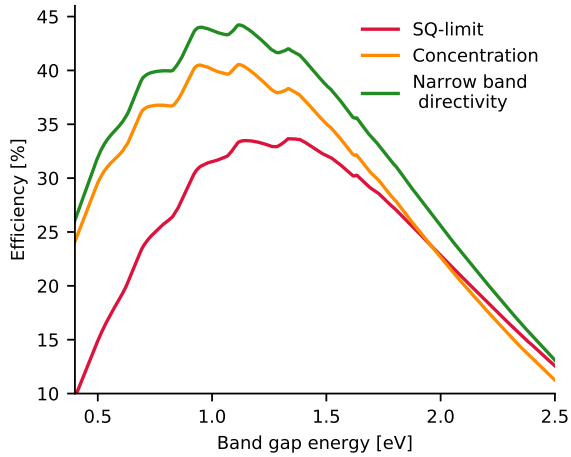

Figure 2.1: Maximum achievable efficiency as a function of bandgap energy based on the AM1.5 spectrum for three models: the SQ limit (blue), maximum concentration of 46200 (orange) and maximum directivity of 46200 over a narrow band width optimized at each bandgap (green). The latter one also captures the diffuse part of the light efficiently.

Any real single junction solar cell under one sun illumination performs below the SQ limit, due to non-radiative recombination of excited electrons. By analyzing the performance of a record efficiency silicon solar cell, we can quantify how much each of the three

loss mechanisms contributes to a reduction in current and/or voltage. For this analysis we assume the solar cell has a stepwise bandgap of 1.1 eV. The amount of non-radiative recombination is given by the photoluminescence quantum yield (PLQY), which is the ratio of radiative recombination to the total (radiative plus non-radiative) recombination. We use a PLQY of 1%, which is the typical value for state-of-the-art silicon solar cells.[34,35] With these assumptions, the modeled cell has an efficiency of 28% under the AM1.5G spectrum. The actual record lies at 26.7%,[36] meaning that other non-idealities that are not considered in this model account for only 1.3%. These are, for example, no ideal stepwise absorption onset and imperfections at the contacts. The remaining difference between the record efficiency and the maximum achievable efficiency of 87%, can be split up in different contributions, as shown in figure 2.2. The fraction of photons that is not absorbed, contains only 19% of the incoming energy. Considering that the conversion efficiency at maximum power generation is 87%, the energy loss due to non-absorbed photons, and thus loss in current, is 16%. The remaining 43% of efficiency loss compared to the maximum power conversion efficiency is due to reductions in voltage, originating from increases in J_0: 5% efficiency loss due to the non-radiative recombination, 12% loss due to isotropic emission and 26% due to thermalization of high energy electrons. In the following sections we will discuss each of the loss mechanisms in more detail, and provide nanophotonic concepts that can help to overcome these losses.

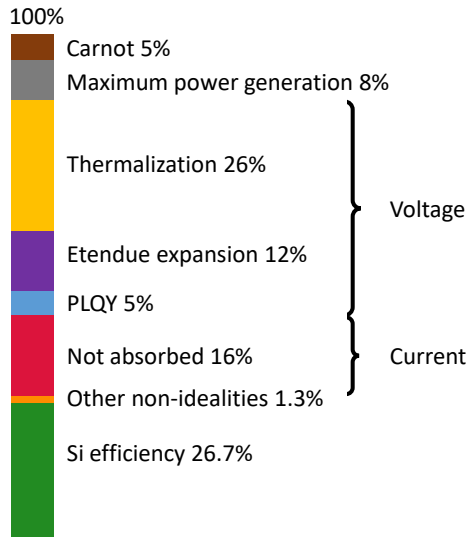

Figure 2.2: Contribution of different loss mechanisms to the total reduction in power conversion efficiency compared to the thermodynamic limit. Most losses (43%) are caused by a reduction in voltage.

2.3 Improving light emission

The reduction in emission intensity due to non-radiative recombination is the first loss mechanism that we will discuss. Any non-radiative recombination increases the saturation current density J_0 and thereby reduces the voltage compared to the radiative limit $V_{oc,rad}$ according to:[33]

$$V_{oc} = V_{oc,rad} + \frac{k_B T}{q} ln\big(PLQY\big), \tag{2.7}$$

The radiative limit is very similar to the SQ limit, but takes into account the realistic, non-stepwise, absorption spectrum. A high performance solar cell should have good absorption anywhere above the bandgap and all of the discussion below assumes that good absorption is achieved. The radiative limit is not approached by reducing J_0 when J_{sc} is not maintained, because efficiency changes only logarithmically with J_0(equation (2.6)), while it changes linearly with J_{sc}.

In approaching the radiative limit, PLQY is the key performance parameter. It is the rate of externally emitted photons divided by the total recombination rate and is determined by two parameters. One is the internal luminescence efficiency Q_i^{lum}, which depends on the radiative and non-radiative rates inside the material. The second is the escape probability p_e: the probability that an internally generated photon makes it to the far field, outside the material. Otherwise it is reabsorbed with probability p_r or parasitically absorbed with probability p_a, such that $p_e + p_a + p_r = 1$. The PLQY expressed in these terms is given by:[33]

$$PLQY = \frac{Q_i^{lum} p_e}{1 - Q_i^{lum} p_r}, \tag{2.8}$$

To approach the radiative limit, we have to maximize Q_i^{lum} and p_e. The internal luminescence efficiency Q_i^{lum} is increased by decreasing the non-radiative recombination rate or by increasing the radiative rate. The probability p_e is increased by improving light outcoupling. Reabsorption in the active material is preferable over parasitic absorption in other materials, so increasing p_r can increase solar cell performance. Once p_a is minimized, p_e should be increased in order to approach the radiative limit.

The non-radiative recombination rate constant is set by the material quality and scales with the density of defects. Nanomaterials can show higher material quality, because they are more easily grown as single crystals. Also lattice mismatch with the substrate is more easily accommodated, allowing for a wider range of materials to be combined. The large surface-to-volume ratio was for a long time considered to be the main drawback of nanomaterials, because many trap states are formed at the surface.[37] However, great progress in surface passivation techniques has led to nanostructures with low non-radiative recombination rates. For example, silicon nanostructures (black silicon) passivated by Al_2O_3[38] or SiO_2,[39] InP nanowires passivated by PO_x[40] and halide perovskite nanowires passivated by porous aluminum oxide templates[41] have all enabled PLQY values comparable to state-of-the-art bulk systems.

Both the radiative recombination rate and light outcoupling can be tuned with nanophotonic engineering. When comparing a planar device to a nanostructured device, many parameters are changed at the same time and it is difficult, if not impossible, to fully separate the different contributions to the final performance. A detailed (mathematical)

analysis is beyond the scope of this paper. We will point out some of the effects that play a role.

The key parameter to which many of the optical properties of nanostructures relate, is the enhancement in light absorption. Initially this was mainly considered as a way to increase J_{sc}. However, it can also improve V_{oc} by increasing PLQY as given in equation (2.7). Absorption enhancement per unit volume leads to a higher density of excited charge carriers inside the material, i.e. higher injection level. The radiative recombination rate scales with the carrier concentration squared, while the trap state assisted non-radiative recombination rate scales only linearly with carrier concentration.[42] The non-radiative Auger recombination scales with carrier concentration cubed and starts to dominate at high injection levels.[42] Therefore Q_i^{lum} usually has a peak at finite carrier concentration; with higher carrier concentration leading to a loss in Q_i^{lum} because of Auger recombination and lower carrier densities leading to a loss because of enhanced trap state assisted non-radiative recombination.[42] Intelligent choice of doping concentrations and absorber layer properties may allow the device to be designed such that the optimum injection level is close to one sun conditions. The effect of enhanced Q_i^{lum} at higher injection levels can also be understood from reciprocity: a higher absorption rate means also a higher emission rate; for the same non-radiative rate this gives an increase in Q_i^{lum}.

Changes in light absorption, and thus light incoupling, will also influence the light outcoupling, and thereby p_e. Intuitively one can understand that when less absorbing material is needed, p_e will be larger in a nanostructured device: emitted light has to travel a shorter distance through the material before it reaches an interface where it can escape. Or again the reciprocity argument can be used: stronger coupling to incoming light, means stronger coupling to outgoing modes, which increases p_e.

The changes in Q_i^{lum} (via enhanced internal radiative rate) and p_e (via enhanced external radiative rate) are related to the same optical effects. Nanostructures can enhance the local density of optical states (LDOS) and they can enhance coupling to specific modes, which is equivalent to locally enhancing the field of incoming waves. Since these effects are coupled and influence both Q_i^{lum} and p_e, these parameters can not be tuned independently. In addition to that, the absorption and emission spectra will be altered by changes in LDOS and electric field strength. Often the consequential changes in V_{oc} are attributed to different parameters in an additive manner, but it has already been shown that in this additive form the different components are not independent.[43] By combining the additive terms in one equation (eq. 27 in[43]) this expression is claimed to contain only independent parameters. However, when considering nanostructures, several terms in this expression are still coupled via the LDOS and field enhancement. A general statement on how these effects change V_{oc} can therefore not be made. However, attempts to attribute changes in V_{oc} to specific parameters has led to some confusion, some of which we will try to resolve here.

In the first place, there is experimental proof of strongly increased V_{oc} and PLQY in nanostructured materials. By comparing a planar InP device to one with nanowires of the same material, an increase in V_{oc} of 70 mV was found due to a combination of enhanced absorption, increased Q_i^{lum} and increased p_e.[28] Light outcoupling enhancement via nanotexturing has also been used to improve methylammonium lead halide perovskite thin film solar cells. For the iodide perovskite, the PLQY was increased by more than a

factor 5, by going from thin film deposition on a smooth glass substrate to a nanotextured substrate.[44] Also without fully quantifying and separating the contributions of the physical processes underlying these effects, it should be clear that nanostructures can improve the optical properties of a material.

One source of confusion is the fact that changing the optical properties of a material can also change the emission and absorption spectrum. This might lead to an effective increase or decrease in bandgap, resulting in a change in $V_{oc,rad}$. When only looking at the resulting voltage, one can come to the conclusion that p_e should be minimized, because this can lead to an effective increase in bandgap and therefore in V_{oc}.[45] However, this is only moving along the bandgap axis in figure 2.1, without actually getting closer to the radiative or SQ limit, as shown by the red arrow in figure 2.3. In the presence of non-radiative recombination, increasing p_e will lead to an increase in PLQY (green arrow in figure 2.3). Even though the absolute V_{oc} may decrease due to a lower effective bandgap, the radiative limit will be more closely approached. Intuitively this can be well-understood from the fact that any reabsorption of a photon (due to a low p_e) provides another chance for non-radiative recombination, which reduces the PLQY. Therefore p_e should always be maximized for approaching the radiative limit as long as absorption is not compromised.

Another source of confusion arises when looking at individual nanoparticles. Instead of an absorption spectrum, they are typically characterized by their absorption cross section σ_{abs} as a function of wavelength, defined as the effective area over which the particle absorbs light. The absorption cross section can be substantially larger than the geometrical size of the particle, which makes the standard definitions for solar cell performance not applicable.[46] In individual nanoparticles, $V_{oc,rad}$ and the radiative recombination rate can be changed over a very large range, which complicates fair comparisons between different systems. In figure 2.3, we show schematically the different situations that can be encountered. When σ_{abs} is increased equally for all wavelengths above the bandgap, the radiative rate is increased. This brings the system closer to the radiative limit, as indicated by the green arrow. As long as σ_{abs} is isotropic, the efficiency can not increase above the radiative limit, because $J_{0,rad}$ (the radiative saturation current density) and J_{sc} are increased by the same amount. To surpass the radiative limit, the expansion of etendue has to be reduced, which is the topic of the next section. This requires an angle dependent σ_{abs}[46] and as a consequence the whole radiative limit moves to higher efficiency for all bandgaps (dotted line). If σ_{abs} is increased more for some wavelengths than for others, the effective optical bandgap of the material is changed and one moves along the bandgap axis, indicated by the red arrow. Depending on whether the starting point is below or above the optimum bandgap, this increases or decreases efficiency. When an individual nanoparticle has a strong resonance at the bandgap, $V_{oc,rad}$ can actually be decreased significantly. The resonance strongly enhances emission and absorption at the bandgap only, by which J_0 is increased much more than J_{sc},[46,47] following the orange arrow. In a full scale solar cell, this would be equivalent to a device with full absorption at the bandgap, but much lower absorption at higher energy. Since a good performing solar cell should have full absorption anywhere above the bandgap, larger absorption rates at the bandgap than at higher energy are not desirable. By designing a structure with a both angular and wavelength-dependent absorption cross section, potentially very high efficiencies can be achieved, as shown by the green curve in figure 2.1. This will be discussed in more detail in the next section.

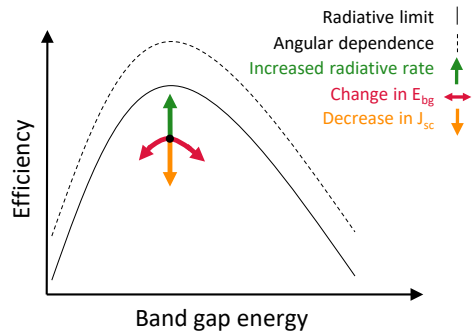

Figure 2.3: Nanostructures can affect the efficiency and V_{oc} in several ways, which occasionally leads to some confusion. Four effects can be distinguished: by enhancing the radiative rate, the PLQY can be increased, approaching the radiative limit (green arrow); the effective bandgap can be changed (red arrow); a resonance at the bandgap effectively decreases J_{sc} and $V_{oc,rad}$ (orange arrow); or the whole radiative limit can be increased by restricting the cone of emission (dotted line).

Throughout this section we have used the PLQY as a measure of solar cell voltage, relying on the reciprocity relation between light absorption and light emission. The critical reader might have noticed that this is technically incorrect, because the reciprocity relation links PLQY to the quasi-Fermi level splitting, while solar cell voltage is connected to the electroluminescence (LED) quantum efficiency. The PLQY and LED quantum efficiency are equivalent when assuming perfect contacts and infinite carrier mobility, but can be different for real materials.[48] However, in mature semiconductor systems, carrier extraction is close to perfect and for most materials, except for organics, the mobility is sufficiently high at one sun fluxes. In this case transport losses do not play a significant role, and the optically and electrically measured quantum efficiency are almost the same.[48,49,50] PLQY is the upper bound and is the one we influence with nanophotonics. We do not focus on carrier transport or carrier injection in this article and therefore use PLQY as a characteristic parameter. Experimentally, PLQY is also often more useful since it can be measured at every step of the solar cell fabrication, while the electroluminescence requires a complete device.

2.4 Matching the angles

The second loss mechanism that we discuss, is the mismatch between absorption and emission angles. This leads to an increase in photon entropy between the incoming and emitted light. Since the conventional SQ limit assumes isotropic emission, this limit can be exceeded by reducing the cone of emission. This leads to a decrease in the radiative recombination $J_{0,rad}$, by which $V_{oc,rad}$, and thus the efficiency, are increased. Emission and absorption are coupled via Kirchhoff's law, so emission into the cone of the sun can not be reduced without sacrificing J_{sc}. The sunlight comes from a cone with a 0.5 degree half angle, which allows for a maximal reduction of J_0 by a factor 46200, compared to emission into the full hemisphere. This corresponds to a maximum increase in voltage of 278 mV.

The most conventional way to reduce the loss due to etendue expansion is by using a concentrating lens. The light that comes directly from the sun is focused onto the cell, while the thermal radiation that comes from all angles is not focused on the cell. Or equivalently, the lens focuses the emission from the cell towards the sun. The resulting efficiency of the SQ limit with 46200 times concentrated AM1.5 spectrum is shown in figure 2.1, orange line. The maximum achievable efficiency is over 40%. However, in a typical terrestrial situation, part of the sunlight is scattered by clouds and surroundings. This light is not focused on the cell and as a consequence the absorption of this diffuse light decreases by the concentration factor. In many terrestrial applications, this decreases J_{sc} more than it increases V_{oc} and the efficiency decreases.

To see the consequences of this effect, we analyzed the impact of diffuse sunlight on conventional concentrating systems. We derived an expression for the relation between efficiency, concentration factor and fraction of direct sunlight. For a concentration factor X, both J_0 and the absorption of diffuse sunlight are reduced by a factor X. Plugging this into the equations for J_{sc} and V_{oc}, and simplifying the expression by neglecting small terms, it can be shown that efficiency approximately scales with concentration factor and fraction of direct sunlight as:

$$\eta \propto J_{sc} f_{dir} \left[ln\left(\frac{J_{sc}}{J_0}\right) + ln\left(f_{dir} X\right) + \frac{1}{X}\frac{1-f_{dir}}{f_{dir}} ln\left(\frac{J_{sc}}{J_0}\right) \right] \tag{2.9}$$

with J_{sc} and J_0 the short circuit and dark current for the cell without concentrating lens, respectively, and f_{dir} the fraction of direct sunlight. The derivation can be found in section 2.8.1. This equation shows that the concentration factor has both a positive ($ln(X)$ term), and a negative ($1/X$ term) effect on efficiency, which originate from the increase in V_{oc} and the decrease in J_{sc}, respectively.

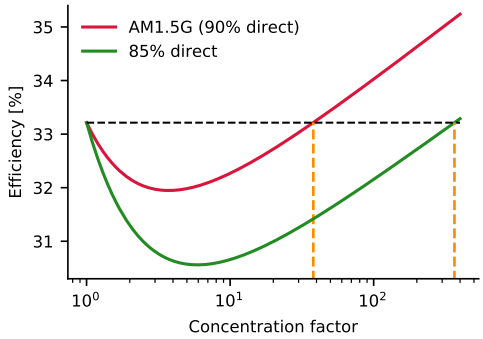

Figure 2.4: Efficiency as a function of concentration factor at a bandgap of 1.11 for different fractions of direct sunlight, calculated with equation (2.9). The black line indicates the efficiency at 1 sun and the orange lines indicate the break even points, above which the efficiency is increased due to the concentration.

We used this expression to calculate the efficiency as a function of concentration factor for a silicon solar cell, ignoring Auger effects. We used a bandgap of 1.1 eV and the AM1.5

spectrum, which contains 90% direct sunlight, and a modified version of this spectrum with 85% direct sunlight. Figure 2.4 shows how at low concentration the reduction in J_{sc} is dominant and the efficiency is decreased. Only above a certain threshold value for X_{thr}, concentration is beneficial. The lower the fraction of direct sunlight, the higher X_{thr} becomes. X_{thr} rapidly increases: by going from 90% to 85% direct sunlight, it increases from 40 to almost 400. Vice versa, the lower the concentration factor, the more direct sunlight is needed. The minimum required fraction of direct sunlight for a given X can be derived from equation (2.9) and reads:

$$f_{dir} = \left[1 + \frac{1}{ln(J_{sc}/J_0)} \frac{X ln(X)}{X-1}\right]^{-1}. \tag{2.10}$$

For the AM1.5 global spectrum, a bandgap of 1.1 eV and maximum concentration (46200x), at least 76% of the sunlight must be direct. For a more practically achievable concentration of 400x, the break-even point lies just below 85% direct sunlight. In many places on earth this value is not reached most of the time. In that case adding a concentrator will make the system perform worse. To get a feeling for the numbers: in the Netherlands the fraction of energy from direct sunlight is on average 36%, in Denver (Colorado, US) this is 76% and in the Sahara this is 80%.[51] The AM1.5G spectrum assumes a clear sky, but still contains 10% diffuse sunlight due to the presence of the atmosphere.

Instead of expanding the angular range of incident sunlight to match the angle of emitted light (as with concentrating lenses described above), it is also possible to reduce the emission angle of the solar cell towards that of the sun. This is done with angle restrictive filters, that block emission and absorption into oblique angles. This concept was described more than two decades ago,[23] and has been studied in order to find upper thermodynamic limits for PV systems since then.[43,52] When acting over the full solar spectrum, angle restrictive mirrors are mathematically equivalent to concentrating lenses and they can be described with an effective concentration factor. However, since emission occurs over a narrow bandwidth, the angle restrictive mirrors can be made wavelength selective. This way, the problem with diffuse sunlight can be circumvented: if the mirrors only block light at the emission wavelength, while they are transparent at higher energy, J_0 is decreased while maintaining high J_{sc}. In practice however, PV systems with angle selective mirrors suffer from the decreased escape probability, which reduces the PLQY as discussed in the previous section(equation (2.8)) as a consequence of photon recycling. The resulting increase in V_{oc} for an effective concentration factor X and initial value of PLQY is given by $(k_B T/q) ln\{X/[X-(X-1)PLQY]\}$, which approaches zero as the initial PLQY goes to zero.[34] This approach was tried experimentally, using a high quality GaAs solar cell. Despite the high PLQY in GaAs the increase in V_{oc} was only a few mV due to the decrease in escape probability.[53]

As mentioned above, concentration and angle restriction are mathematically the same in the radiative limit and without considering diffuse sunlight. When you look at the combined system of solar cell plus concentrating lens or angle restrictor from the outside, both look the same: only incoming light at normal incidence is absorbed and only collimated light comes out. Both techniques have their limitations, and by combining the two losses can be minimized.[24,54] Concentrating lenses always act over the full spectrum, which leads to significant losses in any realistic operating conditions with diffuse sunlight. However,

they do have the advantage of having good light outcoupling, which makes them also applicable to materials with a low PLQY like silicon. Angle restrictors allow for wavelength selectivity, but they work based on reduced light outcoupling. In some cases this can be beneficial, because this light trapping increases the absorption close to the bandgap, increasing Jsc for a given thickness.[55] However, this comes at the cost of increased non-radiative recombination, meaning that the efficiency will always be below the radiative limit for non-ideal materials. Since most work on controlling the emission angles has been focused on angle restricting filters on top of the solar cell, which enhance photon recycling and reduce escape probability, this has led to the misconception that any type of angle restriction only works for solar cells close the radiative limit. With nanophotonic structures this does not have to be the case: they change the emission event itself, instead of interacting with the light after it is emitted. Just like the efficiency of silicon cells can be increased with concentrating lenses, which effectively also change the angular profile of the emission, nanophotonic structures have the potential to improve efficiency also for materials with low radiative efficiency.[21]

Nanophotonic structures can combine the best of both worlds: maintaining high light-outcoupling as with concentrating lenses, while providing wavelength selectivity comparable to angle restriction filters. This requires directive nanoparticles: particles that emit and absorb more in one direction than in all others. This is described by the so called directivity, as used in antenna theory. It is defined as the maximum power absorbed or emitted into a certain direction divided by the average power in all directions. The particles must be directive over a narrow band width around the emission wavelength, and absorb high energy light from all directions. This gives both directive light emission (i.e. reduced emission loss) and good absorption of diffuse sunlight, while maintaining or potentially increasing the escape probability. The resulting efficiency of such system, with the band width of directivity optimized at each bandgap, is shown in figure 2.1, green line.

To achieve these efficiencies, one must have accurate control over the light emission. In the field of nanophotonic engineering several methods have been developed for controlling the emission at the nanoscale. Especially in the field of single photon emitters there is a large demand for increasing the brightness, enhancing the Purcell factor and controlling the directivity.[20] A frequently studied system is the Yagi-Uda antenna. On macroscopic scale this is a well-known antenna design used for radio frequencies. By scaling it down to the nm size, light emission of a single quantum dot can be controlled. Using five gold elements a forward-to-backward ratio of the emission of 4.7 dB has been experimentally achieved.[56] Another well-known geometry is the Bull's eye antenna, which consists of concentric rings or grooves around the emitter(s). With shallow grooves in a gold film a directivity of 7.5 dB was measured from an ensemble of particles.[57] Coupling emitters to plasmonic resonances in an array of aluminum nanoantennas, gave a more than 60-fold directional enhancement for the purpose of efficient light-emitting diodes.[58] By introducing spatial variations in an array of nanoantennas, wavefront shaping with sub-wavelength resolution can be achieved, which is being used for the development of flat optics or metalenses.[59]

All of the above mentioned systems rely on plasmonic nanostructures. The main disadvantage of plasmonic structures is the parasitic absorption in the metals. This realization has led to a shift away from lossy metallic (plasmonic) resonators towards dielectric systems. Here many of the nanophotonic advantages are still present, but without the parasitic

absorption.[60] For example, a hybrid system of a titania Bull's eye structure on a silver film was realized, which gave emission into two lobes with full-width-half-max of 3 degrees.[61] An all-dielectric Yagi-Uda nanoantenna was fabricated from silicon spheres, reaching a maximum directivity above 7 in the microwave range.[62] Also in the field of metalenses the low efficiency associated to the dissipative losses in metals has led to the development of all-dielectric metasurfaces, which show good potential for replacing their plasmonic counterparts.[63]

For the performance of solar cells, parasitic absorption is detrimental for both current and voltage. Initially, work has been done on plasmonic structures for solar cells, mostly to enhance absorption in the solar cell material.[64] Since it became clear that the parasitic absorption in the metals will limit the achievable efficiencies, the attention has now shifted to dielectric nanostructures.[18]

Of course the dielectric materials have their own possibilities and challenges. An advantage is, that dielectric nanoparticles can support both electric and magnetic resonances simultaneously, which can be controlled independently.[60] On the other hand, these resonances are usually less localized than in metals, leading to more broadband response and lower directivity. Fabrication imperfections are challenging in any nanoscale structure and cause sub-optimal geometries and rough surfaces. Insufficient surface passivation has further decreased the performance of dielectric nanophotonic structures so far. Both theoretical and experimental work is to be done on improving light management with dielectric nanostructures and developing pathways to large-scale applications.

A specific example of the kind of design requirements is the angular and wavelength dependent absorption and emission profile needed for the reduction in etendue. For a material with a bandgap at 860 nm (e.g. GaAs), the ideal absorption cross section as a function of angle and wavelength is shown schematically in figure 2.5. The structure must have high absorption at normal incidence, to collect the direct sunlight efficiently, and high absorption from all directions at high energy, to maximize absorption of diffuse sunlight. Close to the bandgap, away from normal incidence the absorption should be low, which makes the emission directional towards the sun. Radiative recombination should be enhanced, while parasitic absorption must be avoided.

To realize such particles, morphologies have to be found and fabricated that lead to anisotropic absorption cross sections. Finding the optimal shape for highly directive particles is a non-trivial nanophotonics problem. Either the absorber material itself can be made into a directive structure, or nanoantennas of dielectric material can be placed around or on top of the semiconductor. The directivity of GaAs nanowires has been increased from 2 to 20 by placing a 'nanolens' on top of the wire. The nanophotonic structure of the lens was designed through an evolutionary algorithm and fabricated using two-photon lithography.[65] For future large-scale application, faster fabrication methods are needed, based on chemical growth or self assembly. A good candidate might be the shape-preserving transformation of carbonate minerals into semiconductors. Carbonate minerals can mineralize into three dimensional shapes in a well controlled manner. Subsequently the structure can be transformed into, for example, methylamonium lead halide perovskite, which is a good solar cell material.[66]

Potentially, high directivities can be reached by combining different effects. For example, it may be possible to place the directive nanolenses in an array that provides additional

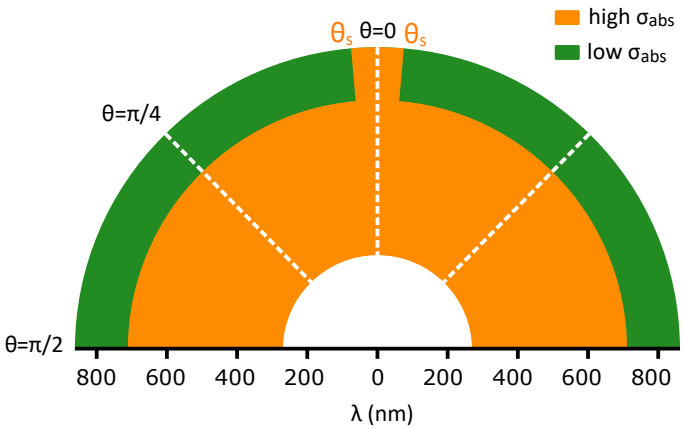

Figure 2.5: Schematic illustration of how the absorption cross section (σ_{abs}) of a nanostructure should vary with wavelength and angle of the incoming light in order to achieve the narrow band directivity. Around the bandgap the nanoparticle should be directive, such that it emits light in the direction of the sun. This requires higher absorption for normal incidence than for oblique angles. At energies further above the bandgap it should absorb light from all directions, to also capture diffuse sunlight.

directivity. Another option is to choose specific emitter materials with intrinsic directional emission, due to preferred dipole orientation[67,68] and combining this with nanolenses or array effects, or both. To achieve the wavelength selective directivity different materials or molecules with specific dipole orientation must be combined and coupled.

2.5 Matching the spectrum

The biggest loss mechanism that applies to all single junction solar cells, is the mismatch in absorption and emission spectrum. For the typical silicon solar cell, as analyzed in figure 2.2, this contributes to an absolute loss of 42% in efficiency. All photons below the bandgap are not absorbed, which accounts for 16% of the loss, and all excess energy of above-bandgap photons is dissipated as heat, thereby losing the remaining 26% of efficiency. There are several techniques available to reduce these losses. In this section we will discus the ones that can benefit from nanophotonics.

A luminescent solar concentrator (LSC) consists of a plate or sheet of transparent material with embedded luminescent particles. These particles absorb the sunlight and subsequently emit light, which is then waveguided through the plate. Small solar cells connected to the waveguide absorb the light and convert it to electricity. Although this system has the name concentrator, it can not increase the efficiency above the SQ limit like the concentrating systems discussed previously. This can be understood from the fact that the thermal emission to the environment is not directed towards the sun, and thus the entropy loss remains. However, LSCs have several advantages, both economical and physical, and nanophotonics can help to improve their performance.

The economical benefit of using an LSC is that the transparent plate with luminescent particles can be cheap and easy to fabricate: existing cover glasses or polymer coatings

used in the solar cell industry can already fulfill the role of a waveguide. The actual solar cells to which the light is guided are very small compared to the collection area. This small size makes expensive, high efficiency solar cells affordable. LSCs can potentially create high efficiency devices, because they can be used in tandem configurations for better capturing of the full solar spectrum. Conventional multi-junction solar cells are complex and expensive to fabricate, because many additional layers are required to accommodate the lattice mismatch, charge transport and surface passivation. The cells are usually connected in series, which limits the current to the lowest current in one of the cells. Stacking LSCs with different bandgaps is less complex, and the cells do not need to be current matched. This makes the tandem less sensitive to temperature and spectral fluctuations and easier to fabricate. Promising results have been found in both theoretical[69] and experimental[70] work on the performance of LSC-tandem configurations.

Nanophotonics engineering is already being used for optimizing the absorption and emission spectra of the luminescent particles in LSCs. With Stokes shift engineering, i.e. the shift between absorption and emission spectrum, reabsorption in the waveguide can be reduced. By properly matching the emission to the absorption of the solar cells, efficiency can be increased. In a tandem configuration the bandgaps of the different layers can be accurately tuned for optimal performance, by using quantum confinement or resonances to change the effective bandgap of the material. However, the main challenge for making high efficiency LSCs is to achieve efficient guiding of the emitted light towards the solar cells. Many photons are often lost along the way, due to non-radiative recombination in the particles, or because they are emitted into the escape cone of the waveguide. The light that is coupled to the waveguide, is often reabsorbed many times along its way. Each reabsorption event leads to another chance of non-radiative recombination or emission into the escape cone.

With nanophotonic engineering, particles can be designed that minimize the losses in the waveguide. By creating directive emission into the plane of the waveguide, the fraction of light emitted into the escape cone can be reduced significantly. It has been proposed to use for example photonic structures to enhance in-plane emission and reduce escape cone losses.[71] By creating aligned directive emission into only one direction, also the chance of reabsorption can be reduced: the structures emit light mostly in one direction (say towards the right), but due to reciprocity they mostly absorb light traveling to the left. This leads to a structure in which light can travel only in one direction. The structure requires a lower directivity than the nanolenses in the previous section: as long as the light is emitted into the cone of total internal reflection of the waveguide, the photons do not escape. The required absorption cross section as a function of angle and wavelength is schematically shown in figure 2.6. Again, at short wavelengths (high energy) the absorption should be high from all directions, to maximize absorption of sunlight, and the particles should be only directive over their emission spectrum.

Another system that reduces the spectral mismatch and that can benefit from nanophotonic engineering, is a photon multiplier. In this concept, high energy photons are converted to two low energy photons. This process takes place in the so-called down converter layer on top of a solar cell, from which the photons have to be emitted towards the solar cell. This down conversion can be realized with singlet fission[72] or multiple exciton generation.[73,74,75] The efficiency of this type of devices can be increased by coupling the down

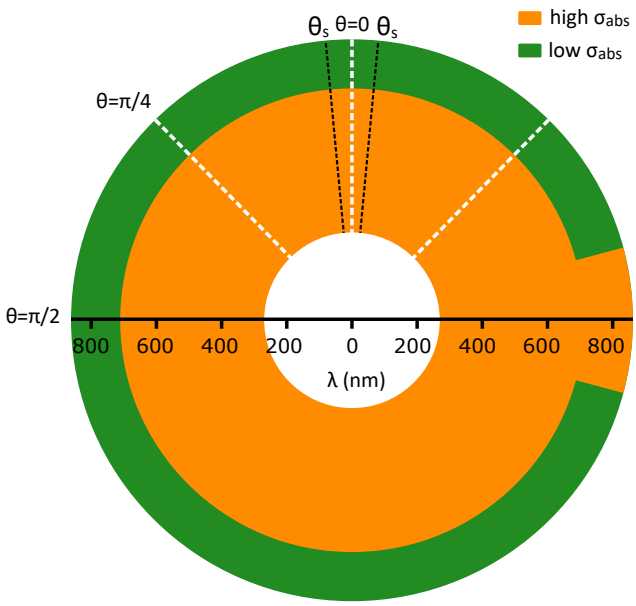

Figure 2.6: Schematic illustration of how the absorption cross section (σ_{abs}) of a nanostructure should vary with wavelength and angle of the incoming light for the emitters in the LSC waveguide. The emission around the bandgap should occur primarily within the cone of total internal reflection, which requires low σ_{abs} in all other directions. At energies higher above the bandgap σ_{abs} should be large to absorb the incoming sunlight from all directions.

converter to directive emitters. This will ensure that the down converted light is emitted towards the solar cell.

Finally, nanostructures can form an alternative configuration for tandem or multi-junction solar cells. Instead of placing layers that absorb different parts of the solar spectrum on top of each other, spectral splitting can be achieved by placing nanostructures next to each other. Thanks to the enhanced absorption cross section of nanowires, adjacent wires with different bandgap can collect light from an overlapping area. Spectral splitting can be achieved by making high bandgap nanowires taller, such that the high energy photons are absorbed before they reach the lower bandgap material wires,[76] or by making use of structures with different resonance frequencies, which cause an enhancement in absorption cross-section at specific frequencies.[77]

2.6 Future solar cells

In this section we propose two concepts for high efficiency solar cell designs, based on the approaches discussed in the previous sections. In the first design, a high efficiency is reached by reducing the cone of emission while maintaining high J_{sc} and p_e by using narrow-band directive nanostructures. The second design combines existing bifacial silicon solar cells with a luminescent solar concentrator, which leads to a low cost, high efficiency tandem device. The performance of each design is evaluated in realistic operating condi-

tions using measured solar spectra, and compared to a more conventional design without nanophotonics.

2.6.1 NARROW BAND DIRECTIVITY NANOLENSES

The first concept aims at a reduction in emission cone, high light outcoupling and good absorption of diffuse sunlight. This is achieved with nanostructures that emit the light into one specific direction, rather than using structures that redirect the light after emission, such that directivity does not come at the cost of light outcoupling. The constituent nanostructures should have an absorption cross section varying with incidence angle and wavelength as shown in figure 2.5. The optimal bandgap for this concept is 1.1eV, as can be seen in figure 2.1. We assume a high quality solar cell material in combination with good light outcoupling to give a PLQY of 85%. This could be achieved with, for example, an alloy of III-V or halide perovskite materials, which provide tunable bandgap and high PLQY. For comparison with state of the art concentrators, we propose a directivity of 400, similar to existing record concentrating solar cells. The optimum band width of the directivity was found to be 0.22 eV, based on simulations with the measured solar spectra. This design is compared with solar cells of the same material (bandgap of 1.1eV and 85% PLQY), without concentration and with macroscopic concentration over the full band width.

With these parameters the performance of the cells can be calculated for any given solar spectrum. The spectra were taken from publicly available measurements from NREL in Denver,[78] measured every 5 minutes throughout the year 2018. Measurements of the direct solar spectra are readily available (SRRL PGS-100 Direct Normal). The diffuse solar spectra could be calculated using the direct spectra, the global horizontal measurements (SRRL WISER Global or Direct) and the azimuth angle of the sun. The temperature of the cell, used in the calculation of J_0, was approximated by the locally measured temperature (Dry Bulb Temperature (deck)). For each spectrum and cell temperature, a detailed balance model is used to determine J_{sc} and J_0, and from these the maximum efficiency is calculated. The results are presented in figure 2.7, showing the increase in efficiency compared to the cell without concentration or directivity, plotted versus fraction of direct sunlight. For low fractions of direct sunlight, macroscopic concentration performs very poorly, as expected from equation (2.10). The efficiency based on annual energy yield is 31.8%, which is a relative decrease of 5% compared to the standard cell (33.6%). This difference is smaller than it might seem from figure 2.7. This is because in general low fractions of direct sunlight correspond to low total incoming power, so the absolute loss in generated power is limited. The narrow band directivity concept outperforms the standard cell over the whole range and the annual energy conversion efficiency is 38.7%, a relative increase of 15% compared to the standard cell. This concept does not suffer from high fractions of diffuse sunlight, which shows the importance of having high directivity only over a narrow band width.

There are still several challenges that need to be solved to realize this concept. As suggested in the section on matching the angles, directive nanostructures can be made in different ways, both from the semiconductor itself or from a dielectric nanolenses on top of the semiconductor. A cheap and fast fabrication technique for directive structures has to be found. A question is whether it is possible to obtain the desired directivity with a texture on a planar film, or by using diffractive effects. Another question is what happens when directive structures are placed in an array and the enhanced absorption cross sections

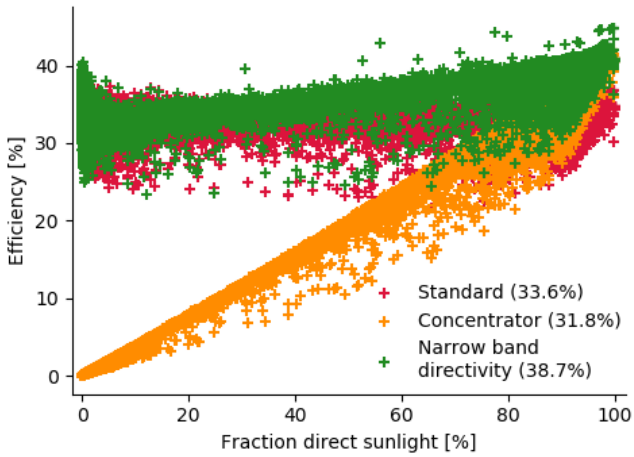

Figure 2.7: Performance of a conventional concentrator system and narrow band directivity system compared to a cell without concentration. The efficiency is plotted as function of the fraction of direct sunlight and the simulations are based on measured solar spectra.[78] The values in brackets indicate the average efficiency over the year. The concentrator reduces the efficiency by 2.7%, while the narrow band directive structures increase efficiency by absolute 7.7%

start to overlap at certain wavelengths or angles. Also fundamental questions need to be solved, to show if there is a limit on directivity in nanostructures or if there is a trade off between directivity, LDOS and light outcoupling. It has to be shown, both theoretically and experimentally, whether the required emission patterns can be achieved. High directivity into a narrow cone requires accurate 2-axis solar tracking: one 'fast' moving rotation to follow the arc of the sun throughout the day and one slow rotation to adjust the axis throughout the year. If a directive structure can be made that emits into a band matching the arc of the sun, tracking throughout the day could be eliminated, allowing for the widely available and inexpensive single axis tracking to be used. These questions and more require further research to nanoscale directivity.

2.6.2 Bifacial LSC-Si tandem device

The second concept aims at combining cheap and well established silicon solar cells with new techniques. We propose a bifacial tandem configuration, where a high bandgap LSC is placed on both sides of a bifacial silicon panel. This concept combines the existing design of silicon cells with a yet to be developed LSC and solves several problems at the same time.

Currently the industry of silicon cells is moving towards bifacial cells, which can also absorb sunlight from the back side. This can give a significant increase in energy output per panel, especially in regions with large fractions of diffuse sunlight. To increase energy output even further, the efficiency has to be increased. As discussed in relation to figure 2.2, silicon solar cells perform close to their limit, and improving efficiency requires new measures. The biggest gain can be found in going to a tandem configuration, with a high

bandgap material on top of the silicon. As mentioned before, conventional tandem cells are expensive to fabricate and suffer from current matching. Using an LSC can potentially be a very cheap solution. Standard silicon solar cells already have a encapsulation layer, that could serve a dual purpose as an LSC, without adding a fabrication step to the module assembly. Currently existing LSCs suffer from low efficiency and this is the main challenge that might be solved with directional emission from nanostructures in the LSC.

A typical solar cell module consists of an array of silicon wafers. For monocrystalline silicon, these wafers are cut from a cylindrical ingot. The packing efficiency in a panel is increased by cutting the circular wafers into squares. To limit the waste of material, the squares are cut slightly too big, which leads to 'missing' corners that are typically visible on the modules. We propose to place the high bandgap cells of the LSC in these empty squares of the module. For standard silicon cells used in industry (commonly called 6-inch wafers) the missing corners form a fraction of 0.6% of the total area. This gives a concentration factor of 170 for the LSC. In figure 2.8 the layout is shown schematically. For the small, high bandgap cells, high efficiency III-V materials can be used. These are expensive, but the concentration of the LSC reduces the price by factor 170. By placing them in between the c-Si cells, there is no need for lattice matching or wafer bonding.

Aligned directive nanostructures, with an absorption cross section as depicted in figure 2.6, are used to optimize emission into the waveguide and to minimize reabsorption. The exact requirements on the absorption cross section depend on several parameters, like the refractive index of the waveguide (and thus the escape cone), the PLQY of the emitters, the Stokes shift and the scattering cross section. Fully modeling this is beyond the scope of this paper. A simple parameter that captures several effects is the internal efficiency Q_{int} that gives the ratio of the number of photons that reach the LSC solar cells compared to the number of photons absorbed in the LSC (sometimes also called the optical quantum efficiency in the LSC community). This parameter accounts for the major loss mechanisms in an LSC: photons escaping the waveguide and photons lost due to non-radiative recombination, including the effects of reabsorption along the way. We use this parameter to take into account the directive emission in the modeling of the performance of the LSC-tandem concept: a high Q_{int} corresponds to high directivity, because this reduces reabsorption and escaping of photons.

To simulate the performance of this concept, several parameters have to be quantified. For the bifacial silicon cell a PLQY of 1% and a step wise bandgap of 1.1eV are assumed. The optimum bandgap of the LSC was found to be 1.75 eV through optimization with measured solar spectra. The high bandgap cells are modeled to have an PLQY of 85%. Different values of Q_{int} have been evaluated. If less than three quarters of the photons absorbed in the LSC are collected, it performs worse than the current matched tandem. If less than half of the photons are collected, the performance is worse than only the bifacial silicon cell. Here we model the performance of a system with Q_{int} = 90%. We assume that the back side of the bifacial cell receives 75% of the diffuse sunlight. For a bifacial silicon panel without LSC this gives a yearly increase in energy output of 15%, compared to a monofacial cell. Some long running field tests with bifacial cells have shown an increase between 10% and 20%, so the increase of 15% is a realistic approximation.[79] The performance of the LSC-Si tandem is compared with a current matched tandem, with the same bifacial silicon bottom cell, but no tandem on the back. The top cell has again a bandgap of 1.75eV and an PLQY of 85%.

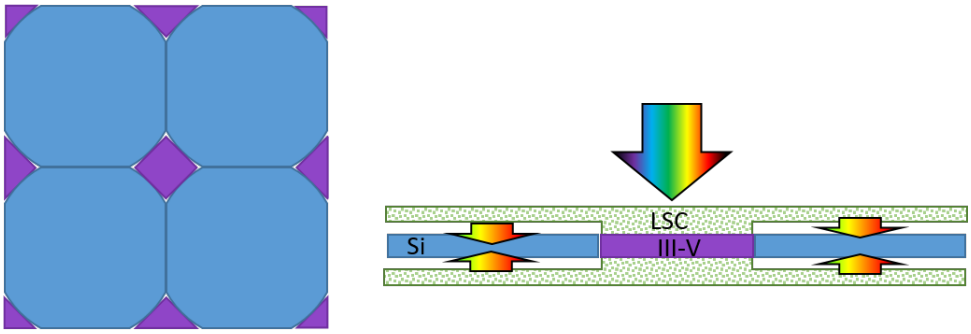

Figure 2.8: Schematic layout of the LSC-Si tandem configuration, where the high bandgap cells sit in the gaps between the silicon wafers. The connection between the LSC and the small solar cells must be index matched, such that the waveguided light leaks out and couples into the cell.

With these assumptions the performance is again calculated based on the measured solar spectra[78] by simulating the tandem devices in a detailed balance model. The results of the simulation are shown in figure 2.9, where the performance is plotted relative to a single junction bifacial cell. In this case the efficiency is plotted versus the mean wavelength of the spectrum. Spectral shifts reduce the performance of current matched tandem, because the current is determined by the minimum current in either of the two cells. If the spectrum is red-shifted, the current in the high bandgap cell decreases. The blue shifted spectra correspond to high fractions of diffuse sunlight. In this case the reduced current in the Si bottom cell due to the blue-shift, is compensated with the contribution of diffuse sunlight on the back side and the efficiency remains high. The yearly energy output compared to standard bifacial panel is increased by an absolute 9.2%, which is a 28% relative increase.

The bifacial LSC-tandem configuration exceeds the performance of the two others at almost every spectrum. The yearly energy output is increased by 13.3% compared to the single junction bifacial cell and 4.1% compared to the current matched tandem, relative increases of 41% and 10% respectively. It benefits from the increased efficiency of a tandem device, without current losses and with less complex manufacturing. This shows the great potential of optimized LSC-tandem configurations.

The performance of the systems is given as a relative efficiency compared to a reference bifacial cell. We want to mention that the efficiency of a bifacial device is ill-defined without specifying the environment around the cell, PV packing density, and other geometric factors. The great benefit of bifacial configurations is the fact that they can harvest diffuse sunlight that is scattered from elsewhere. When the efficiency is calculated based on the incident sunlight per unit area, this can lead to apparently very high efficiencies at high fractions of diffuse sunlight, because light is effectively harvested from a larger area. This leads to seemingly unrealistic results when reporting absolute efficiencies, and therefore it is more insightful to look at the relative performance of the three systems.

For this concept the same questions apply regarding directive nanostructures as for the first design. A detailed modeling of the aligned nanolenses in a waveguide must be done to show whether asymmetric transmission can be achieved. One possible problem could

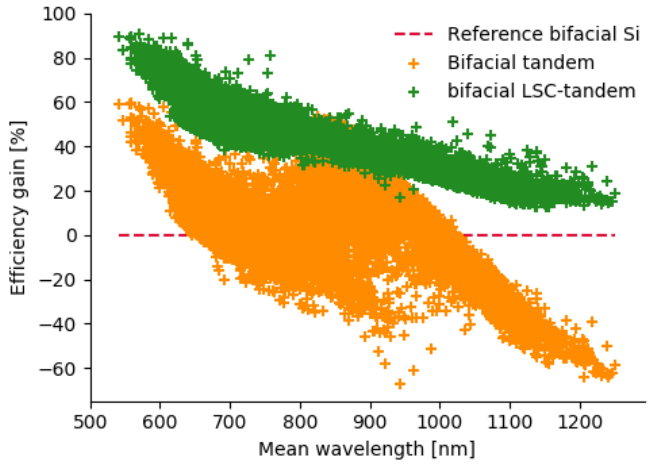

Figure 2.9: Relative performance of a bifacial current matched tandem and a bifacial LSC-tandem configuration compared to a bifacial silicon solar cell. The relative performance is plotted as function of the mean wavelength in the spectrum and the simulations are based on measured solar spectra.[78] The current matched tandem and the LSC tandem show an absolute increase of 9.2% and 13.3% in power generation compared to the bifacial silicon cell, respectively.

be the scattering of light in undesired directions, but some preliminary modeling showed that the transmission of directive nanolenses is high and that less than 10% of the light incident on the back (low absorption) side is scattered backwards. Furthermore techniques need to be developed to make waveguides with aligned nanostructures and couple them to solar cells.

2.7 Conclusion

In this Perspective article we gave an overview of how nanomaterials can increase solar cell efficiency. Nanomaterials have a great potential due to their strong and tunable interaction with light, originating from their size being comparable to the wavelength of light. This allows for controlling the emission event itself, instead of manipulating the light after it has been emitted, which is a key difference compared to macroscopic approaches. In this article we covered the different aspects in which nanomaterials can play a role in increasing solar cell efficiency. To do so we took a step back and looked at the fundamental properties needed to make a good solar cell. From thermodynamics we learned that an ideal solar cell in open circuit should emit all light back to the sun. This shows the importance of good light management, not only to optimizing absorption, but also making good, defect-free materials and applying nanophotonic engineering to accurately control the emission. By comparing a typical silicon solar cell to the idealized thermodynamic model we identified three differences in the emitted light: the spectral band width, the intensity and the angular emission profile. Each of these cause a reduction in V_{oc}, while J_{sc} is only mildly affected. This is also seen in record solar cells: while J_{sc} approaches the theoretical

limit, V_{oc} is typically lagging behind. This perspective focuses on ways to increase V_{oc} with nanomaterials, because this field has only recently emerged and is rapidly developing.

For each of the three loss mechanisms we gave an overview how nanomaterials can help in reducing the losses. We have pointed out what has been achieved so far and what the remaining challenges are. Finally we applied this knowledge in two conceptual solar cell designs. We showed that with nanostructures that reduce the cone of emission while maintaining sensitive to diffuse light, the performance in terrestrial application can be increased by 15%. A conventional, macroscopic solution will actually decrease performance by 8% due to its low performance in the presence of diffuse sun light. A bifacial LSC-tandem configuration based on nanophotonic structures can increase performance compared to a bifacial silicon cell by 41%, while a more conventional current matched tandem gives an increase of 28%. Further development in designing and fabricating nanostructures for accurately optimized light management has the potential for contributing to high efficiency solar cells at low cost.

2.8 Supporting information

2.8.1 Derivation of effect of concentration

The maximum efficiency of a solar cell is given by the power output devided by the incident solar power. The power output is given by the product of the V_{oc}, J_{sc} and the fill factor. In this approximation we will only consider the effect of concentration on V_{oc} and J_{sc}, so we can write:

$$\eta \propto V_{oc} \cdot J_{sc} \tag{2.11}$$

The open circuit voltage scales with the logarithm of J_{sc} over J_0:

$$V_{oc} \propto ln(\frac{J_{sc}}{J_0}), \tag{2.12}$$

and J_{sc} and J_0 are finally the ones that depend on the concentration factor X:

$$J_{sc} = J_{dir} + \frac{J_{dif}}{X}, \tag{2.13}$$

where J_{dir} is the photon current corresponding to the photon flux of direct sunlight, and J_{dif} the photon current corresponding to the photon flux of diffuse sunlight. A concentrating lens or angle restriction filter blocks part of the diffuse sunlight, decreasing it with a factor X. The dark current J_0 is as a whole reduced by factor X:

$$J_0 = \frac{J_{0,0}}{X} \tag{2.14}$$

Filling in equations (2.12) to (2.14) into equation (2.11) gives:

$$\eta \propto ln\left(\frac{J_{dir} + \frac{J_{dif}}{X}}{\frac{J_{0,0}}{X}}\right) \cdot \left(J_{dir} + \frac{J_{dif}}{X}\right) \tag{2.15}$$

We assume that the fraction of current due to direct sunlight is proportional to the fraction of direct sunlight, such that the fraction of direct sunlight f_{dir} can be calculated as:

$$f_{dir} = \frac{J_{dir}}{J_{sc,0}}, \tag{2.16}$$

J_{dif} and J_{dir} always add up to $J_{sc,0}$, the total current without concentration, such that $J_{dif} = (1 - f_{dir})J_{sc,0}$. This allows us to write equation (2.15) as

$$\eta \propto ln\left(\frac{f_{dir}J_{sc} + \frac{(1-f_{dir})J_{sc}}{X}}{J_0/X}\right)\left(f_{dir}J_{sc} + \frac{(1-f_{dir})J_{sc}}{X}\right) \tag{2.17}$$

Reorganizing the terms gives:

$$\eta \propto f_{dir}J_{sc,0}\left[ln\frac{J_{sc}}{J_0} + ln(f_{dir}X + 1 - f_{dir})\right]\left(1 + \frac{(1-f_{dir})}{f_{dir}}\frac{1}{X}\right) \tag{2.18}$$

The value of f_{dir} is smaller than 1, while X is always equal to or larger than one. In most cases $X \gg r$, so for typical values of $J_{sc,0}/J0,0$, we can simplify equation (2.18) by assuming $ln(f_{dir}X + 1 - f_{dir}) \approx ln(X)$ to get:

$$\eta = f_{dir}J_{sc,0}\left[ln\left(\frac{J_{sc,0}}{J_{0,0}}\right) + ln\left(f_{dir}X\right)\right]\left[1 + \frac{1-f_{dir}}{f_{dir}}\frac{1}{X}\right] \tag{2.19}$$

Working out the brackets and noting that $\frac{1}{X}ln(X)$ is much smaller than the other terms we get

$$\eta \propto J_{sc}f_{dir}\left[ln\left(\frac{J_{sc}}{J_0}\right) + ln\left(X\right) + \frac{1}{X}\frac{1-f_{dir}}{f_{dir}}ln\left(\frac{J_{sc}}{J_0}\right)\right] \tag{2.20}$$

The validity of the simplifications was checked by comparing the outcome of this expression with a numerical simulation. The resulting efficiency with increasing the concentration factor was calculated for a bandgap of 1.1 eV with the AM1.5 spectrum, which contains ca. 90% direct sunlight. The result is shown in figure 2.10, with in blue the efficiency as calculated numerically with a Shockley-Queisser type of calculation, and in orange the outcome of the analytical expression of equation (2.20). The two calculations show good agreement, so equation (2.20) can be used to draw conclusions about the performance of concentrating systems in terrestrial applications.

2.8.2 Modeling of solar cells under realistic operating conditions

Data preparation

From the NREL website the following data sets were downloaded:

- Direct solar spectra: SRRL PGS-100 Direct Normal
- Global horizontal spectra: SRRL WISER Global or Direct
- Temperature: Dry Bulb Temperature (deck)
- Zenith angle of the sun using the free calculation tool

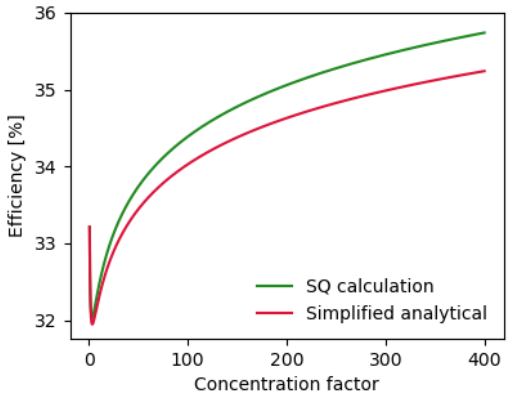

Figure 2.10: Efficiency as a function of concentration factor at a bandgap of 1.11 for the AM1.5 spectrum, blue line corresponds to the numerical SQ-calculation, orange is the results of equation (2.20)

The solar spectra are taken every 5 minutes, while the temperature data set contains measurements every minute. Also some data points are missing in the solar spectra data sets. A script was written that matches the four data sets and keeps only those data poins that are present in all four data sets.

The direct solar spectra run from 334 nm to 1075.4 nm. The global horizontal spectra run from 290nm to 1650nm. To obtain realistic values for the calculated efficiency, the spectra should contain higher wavelengths, like the AM1.5 spectrum that runs to 4000nm. Therefore the long wavelength tail of the AM1.5 spectrum is appended to the measured spectra, weighted by the average power in the last 100 data points of the measured spectra (i.e. 1000 to 1075 nm for the direct spectra and 1550 to 1650 nm for the global spectra). After appending this long wavelength tail, all spectra are interpolated over the wavelength range from 334 to 4000 nm at 1 nm step size.

Efficiency modeling

The efficiency is calculated based on the Shockley-Queisser model. Using the equation:

$$J = J_0(e^{\frac{qV}{k_B T}} - 1) - J_{sc} \tag{2.21}$$

The J-V curve is constructed for a given J_{sc} and J_0. The efficiency is calculated from the maximum power point and the given input power. J_0 is calculated by integrating the photon flux of the black body emission spectrum above the bandgap, assuming a step wise bandgap. J_{sc} is calculated as the integral over the solar spectrum at all energies above the bandgap in terms of photon flux.

The standard cell J_{sc} is calculated from the sum of the direct and the diffuse spectrum. For the conventional concentrator, the contribution of diffuse sunlight is reduced by the concentration factor X, and J_0 is reduced by factor X. For the narrow band directivity model, only J_0 is reduced by factor X.

For the bifacial silicon cell, J_{sc} is calculated using a total incoming flux of the direct sunlight plus 175% of diffuse sunlight, corresponding to 75% diffuse sunlight on the back side.

For the current matched bifacial tandem, the top cell receives just the sum of the direct and diffuse spectra. The silicon bottom cell receives all that is not absorbed by the top cell, plus 75% of the diffuse spectra from the back. In the LSC model the high bandgap cell is on both sides and receives the direct plus 175% diffuse light and the silicon cell receives everything that is not absorbed in the top cells.

The fraction of diffuse sunlight is calculated from the incoming power in the spectra, weighted by the total incoming power. The mean wavelength is calculated with:

$$\lambda_{mean} = \frac{\int P(\lambda)\lambda \, d\lambda}{\int P(\lambda) d\lambda} \tag{2.22}$$

where $P(\lambda)$ is the spectrum in watts per square meter per wavelength.